IET Radar, Sonar & Navigation

Research Article

IET Journals
The Institution of Engineering and Technology

Orthogonal frequency division multiplexing linear frequency modulation signal design with optimised pulse compression property of spatial synthesised signals

ISSN 1751-8784
Received on 18th December 2015
Accepted on 26th February 2016
E-First on 5th May 2016
doi: 10.1049/iet-rsn.2015.0642
www.ietdl.org

Hui Li[1] ✉, *Yongbo Zhao*[1], *Zengfei Cheng*[1], *Da-Zheng Feng*[1]

[1]*National Laboratory of Radar Signal Processing, Xidian University, Xi'an, People's Republic of China*

✉ *E-mail: lihui1990happy@126.com*

Abstract: Orthogonal frequency division multiplexing (OFDM) linear frequency modulation (LFM) waveform is widely studied due to its application potentials in multiple-input–multiple-output (MIMO) radar, but its effective design is still a challenge. Considering the critical role, the pulse compression property of spatial synthesised signals plays in MIMO radar, a detailed analysis is made using OFDM LFM signals, resulting in the radical reasons for the high grating sidelobes. Then, a joint optimisation method for OFDM LFM signal design based on genetic algorithm and sequential quadratic programming is proposed to degrade the sidelobe level dramatically. Furthermore, to nullify the grating sidelobes thoroughly, a modification is performed through optimising the relaxed frequency steps of the OFDM LFM waveform, which involves a balance between sidelobe property and orthogonality. Numerical results validate the theoretic analysis and show the superior performance of the designed OFDM LFM waveforms in pulse compression properties of spatial synthesised signals.

1 Introduction

Multiple-input–multiple-output (MIMO) radar consists of multiple transmit antennas and receive antennas, and each transmit antenna can choose the transmitted waveform freely. It has been shown that this kind of radar system has many advantages such as enhanced flexibility, improved parameter identifiability and excellent interference rejection capability [1–3] etc.. To obtain the merits mentioned above, some properties of the transmitted waveforms are necessary, e.g. good Doppler tolerance [4–6], perfect orthogonality [7, 8], large time-bandwidth product [9] and superior correlation property [10–12]. Thus, some waveforms have been specially designed to improve some of these properties [5–12]. Among them, orthogonal frequency division multiplexing (OFDM) linear frequency modulation (LFM) waveform, which is widely used in communication systems, has favourable Doppler tolerance and large time-bandwidth product, and hence is suitable for radar application [13–20].

Research on OFDM LFM waveform design has attracted much attention in recent years. An OFDM radar signal for detecting a moving target in the presence of multipath reflections was designed [14]. To improve the radar's wideband ambiguity function, an adaptive technique was proposed to design the spectrum of an OFDM waveform [15]. According to the application on MIMO radar, a novel OFDM chirp waveform design scheme consisting of the modulation and demodulation algorithm was proposed [16], and further it is employed with digital beamforming to establish the multimodal operation concept for MIMO synthetic aperture radar [17]. However, the correlation property or ambiguity function was not considered adequately, and the orthogonal waveforms should be generated at the cost of the chirp repetition. In [18], random matrix modulation was applied to produce multiple OFDM LFM waveforms. Though these design issues and processing techniques provide solutions to generate OFDM LFM waveforms, the pulse compression properties of spatial synthesised signals were not studied.

In fact, the spatial synthesised signals of the OFDM LFM waveform have poor pulse compression property, i.e. the high grating sidelobes, which leads to the poor performance in target detection for practical application, e.g. the false alarm and the weak target embedded. Thus, some methods were proposed to solve this problem in recent decade. In [19], Dai *et al.* studied the ambiguity function of OFDM LFM waveform with unlapped frequency band, and also proposed some methods to suppress the sidelobes such as the alternative transmission scheme, the extended matched filter and the windowing processing. In [20], the parameter setting problem was discussed, and it was mentioned that the correlation properties of overlapped OFDM LFM waveform are different from that of the unlapped waveform, which can suppress the sidelobe level infinitely. However, the further optimisation on correlation properties of the overlapped OFDM LFM waveform is not included in [20].

Similar to OFDM LFM in MIMO radar which is the frequency division in transmit antennas, stepped frequency LFM pulses [21] implement the frequency division in transmit pulses and also has the problem of high sidelobes. Methods such as destroying the periodicity [22, 23], using non-linear modulation [24] or setting relationship between waveform parameters [25] to further lower the sidelobes were discussed. However, the stepped frequency LFM signal is one signal with different carrier frequencies in the pulses; hence, these methods cannot be adopted to OFDM LFM waveform design directly.

Up to now, the radical reason for the high grating sidelobes of the OFDM LFM waveform is not reported, and the existing waveform design methods only concern the signal processing techniques, parameter setting etc., whereas few objective optimisation techniques are proposed to design the OFDM LFM waveform with good pulse compression property of spatial synthesised signals. In this paper, we point out the essential causations for the grating sidelobes and propose some optimisation methods to suppress or eliminate them. Specifically, a joint optimisation method based on genetic algorithm (GA) [26, 27] and sequential quadratic programming (SQP) [28] is proposed to search for the optimal frequency codes and the initial phase vector alternately. Compared with the existing waveforms, the resulting waveforms have much lower sidelobe level, perfect orthogonality and constant envelope, but the sidelobes are still discrete and false detection may exist. To eliminate the discrete sidelobes thoroughly, a modification which relaxes the constraints on frequency codes is presented. Unlike the initial joint optimisation method mentioned above, the spatial property should be considered since the relaxation affects the orthogonality. The obtained waveforms realise the nullification of the grating sidelobes at little expense of

orthogonality. Theoretical analysis and simulation results verify the improved correlation properties of the designed waveforms, which result in the enhanced performance in target detection.

The rest of this paper is organised as follows. MIMO radar signal model based on OFDM LFM waveform is introduced in Section 2. In Section 3, an analysis is made of the pulse compression property of spatial synthesised signals. Section 4 proposes a new algorithm of joint optimisation method, as well as the modification. Design results are presented and discussed in Section 5 to verify the proposed methods. Finally, some conclusions are drawn in Section 6.

2 MIMO radar signal model based on OFDM LFM

The transmit antennas in MIMO radar can transmit signals with different carrier frequencies which are called OFDM-coded waveform. Replacing the fixed-frequency signals with LFM signals, OFDM LFM waveform is proposed. An OFDM LFM waveform set consisting of M signals can be represented as

$$\left\{s_m(t) = a(t)\mathrm{e}^{\mathrm{j}2\pi\left(f_m t + (1/2)\mu t^2\right)}\right\}, \quad m = 1, 2, \ldots, M \tag{1}$$

where $a(t) = \begin{cases} 1, & -T/2 \le t \le T/2 \\ 0, & \text{else} \end{cases}$ is the rectangular window of unit amplitude and duration T, T is the time duration of $s_m(t)$. $\mu = B_S/T$ is the chirp rate, where B_S is the modulation bandwidth of the single LFM signal. $f_m = f_0 + c_m\Delta f$ is the carrier frequency of the mth chirp signal with centre frequency f_0, frequency step Δf and frequency code c_m. The available bandwidth of the OFDM LFM waveform is $B = B_S + (M-1)\Delta f$. Particularly, the frequency step Δf is selected as $\Delta f = q/T$, where $q = 1, 2, \ldots, \lceil (B - B_s)/(M-1) \rceil$ is a positive integer, so that any two LFM signals are orthogonal. The centre frequency f_0 is set to zero in this paper without loss of generality.

Consider a collocated narrowband MIMO radar system with M transmitters. The transmit array is a uniform linear array with inter-element-spacing d and transmission wavelength λ. Assume that there is a target located at angle θ, then the spatial signal synthesised at the target is

$$\begin{aligned} y(\theta, t) &= \boldsymbol{a}_t^{\mathrm{T}}(\theta)\boldsymbol{S}(t) \\ &= \sum_{m=1}^{M} \mathrm{e}^{\mathrm{j}2\pi(m-1)d\sin(\theta)/\lambda} s_m(t) \end{aligned} \tag{2}$$

where $\boldsymbol{a}_t(\theta) = \left[1, \mathrm{e}^{\mathrm{j}2\pi d\sin(\theta)/\lambda}, \ldots, \mathrm{e}^{\mathrm{j}2\pi(M-1)d\sin(\theta)/\lambda}\right]^{\mathrm{T}}$ is the transmit steering vector, $(\cdot)^{\mathrm{T}}$ denotes the transpose of a matrix and $\boldsymbol{S}(t) = [s_1(t), s_2(t), \ldots, s_M(t)]^{\mathrm{T}}$ represents the vector of M transmitted signals.

Following (2), the average power received at the location θ is:

$$\begin{aligned} P(\theta) &= \frac{1}{T}\int_0^T |y(\theta, t)|^2 \,\mathrm{d}t \\ &= \frac{1}{T}\int_0^T \boldsymbol{a}_t^{\mathrm{T}}(\theta)\boldsymbol{S}(t)\boldsymbol{S}^{\mathrm{H}}(t)\boldsymbol{a}_t^{*}(\theta)\,\mathrm{d}t \\ &= \boldsymbol{a}_t^{\mathrm{T}}(\theta)\boldsymbol{R}\boldsymbol{a}_t^{*}(\theta) \end{aligned} \tag{3}$$

where $\boldsymbol{R} = (1/T)\int_0^{\mathrm{T}}\boldsymbol{S}(t)\boldsymbol{S}^{\mathrm{H}}(t)\,\mathrm{d}t$ is the covariance matrix of transmitted signals and $(\cdot)^*$ denotes the conjugate. It is shown that if the transmitted signals are orthogonal, the powers received in all directions are equal, which has some advantages in target searching and detection. According to the signal processing structure for MIMO radar [29], the result of space–time matched filter following receive beamformer is:

$$f(\theta, \theta_h, \tau) = \int_{-\infty}^{\infty} y(\theta, t)y^*(\theta_h, t-\tau)\,\mathrm{d}t \tag{4}$$

where τ is the delay time and θ_h is the beam direction. If $\theta_h = \theta$, (4) is the pulse compression result which is equivalent to the autocorrelation function of the spatial synthesised signal; otherwise, it is the cross-correlation function of the signals seen at two different locations.

The properties of $f(\theta, \theta_h, \tau)$ have a great influence on target detection, e.g. the high autocorrelation sidelobe results in false detection, the high cross-correlation levels may cause interferences between the echoes of different targets. Considering the effect of receive beamforming beforehand, it is the autocorrelations that mainly act on the target detection. To obtain fine pulse compression property for target detection, the direct way is to analyse and optimise the autocorrelation function in (4), which is written as $f(\theta, \tau)$ for concision. It is the goal of this paper.

3 Pulse compression analysis of spatial synthesised signal

On the basis of the signal model described in Section 2, the pulse compression of spatial synthesised signal will be analysed in detail, which results in the reasons for the grating sidelobes. The result of pulse compression is as (see (5)) where

$$\begin{aligned} \zeta_u(\tau) &= \int_{-\infty}^{\infty} a(t)a(t-\tau)\mathrm{e}^{\mathrm{j}\pi\left[\mu t^2 - \mu(t-\tau)^2\right]}\mathrm{e}^{\mathrm{j}2\pi u t}\,\mathrm{d}t \\ &= a(\tau/2)\frac{\sin[\pi(\mu\tau + u)(T - |\tau|)]}{\pi(\mu\tau + u)(T - |\tau|)}(T - |\tau|)\mathrm{e}^{\mathrm{j}\pi u\tau} \end{aligned} \tag{6}$$

$$R_v(\tau) = \sum_{m=v+1}^{M} \mathrm{e}^{\mathrm{j}2\pi f_{m-v}\tau}\mathrm{e}^{\mathrm{j}2\pi v d\sin(\theta)/\lambda}\zeta_{f_m - f_{m-v}}(\tau) \tag{7}$$

$$Z_n(\tau) = \sum_{m=1}^{M-n} \mathrm{e}^{\mathrm{j}2\pi f_{m+n}\tau}\mathrm{e}^{-\mathrm{j}2\pi n d\sin(\theta)/\lambda}\zeta_{f_m - f_{m+n}}(\tau) \tag{8}$$

and $u \in \{f_k - f_l,\ k = 1, 2, \ldots, M,\ l = 1, 2, \ldots, M\}$. The first term of (5) describes the mainlobe, whereas the last two terms characterise the left sidelobes and right sidelobes. Owing to the symmetry between $\sum_{v=1}^{M-1} R_v(\tau)$ and $\sum_{n=1}^{M-1} Z_n(\tau)$, and the similarity of their $M-1$ items, the properties of $f(\theta, \tau)$ can be seen clearly through analysing only the item $R_v(\tau)$ or $Z_n(\tau)$.

Usually, the frequency code c_m is set to $m - (M+1)/2$. Thus, the mth carrier frequency becomes $f_m = c_m\Delta f = [m - (M+1)/2]\Delta f$ and (7) can be written as

$$R_v(\tau) = \sum_{m=v+1}^{M} \mathrm{e}^{\mathrm{j}\pi(2c_m - v)\Delta f\tau}\mathrm{e}^{\mathrm{j}2\pi v d\sin(\theta)/\lambda}\chi_{v\Delta f}(\tau) \tag{9}$$

where

$$\chi_{v\Delta f}(\tau) = a(\tau/2)\frac{\sin[\pi(\mu\tau + v\Delta f)(T - |\tau|)]}{\pi(\mu\tau + v\Delta f)(T - |\tau|)}(T - |\tau|) \tag{10}$$

Take the absolute value of (9) as

$$|R_v(\tau)| = \left|\chi_{v\Delta f}(\tau)\right|\left|\sum_{m=v+1}^{M} \mathrm{e}^{\mathrm{j}\pi(2c_m - v)\Delta f\tau}\mathrm{e}^{\mathrm{j}2\pi v d\sin(\theta)/\lambda}\right| \tag{11}$$

Equation (11) is a product of two terms. The first term is a sinc-like function whose maximum value $T - |\tau_1|$ arises at $\tau_1 = -v\Delta f/\mu$. The second term

$$\begin{aligned} |W_v| &= \left|\sum_{m=v+1}^{M} \mathrm{e}^{\mathrm{j}\pi(2c_m - v)\Delta f\tau}\mathrm{e}^{\mathrm{j}2\pi v d\sin(\theta)/\lambda}\right| \\ &= \left|\mathrm{e}^{\mathrm{j}2\pi v d\sin(\theta)/\lambda}\frac{\sin[\pi(M-v)\Delta f\tau]}{\sin[\pi\Delta f\tau]}\right| \\ &= \left|\frac{\sin[\pi(M-v)\Delta f\tau]}{\sin[\pi\Delta f\tau]}\right| \end{aligned} \tag{12}$$

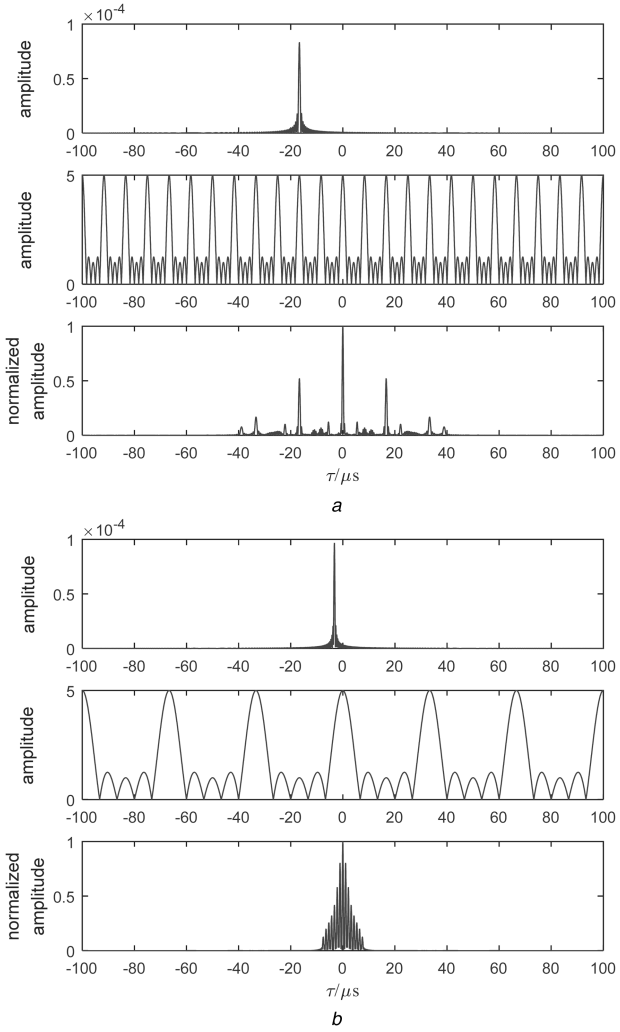

Fig. 1 *Pulse compression analysis of spatial synthesised signals with* $|\chi_{v\Delta f}(\tau)|$, $|W_v|$ *and* $|f(\theta, \tau)|$ *at top, middle and bottom, respectively, where* $v = 3$, $T = 100$ μs, $B = 3$ MHz, $M = 8$, $d = \lambda/2$ *and* $\theta = 30^\circ$
a $T\Delta f = 12$
b $T\Delta f = 3$

is a periodic function which has $T\Delta f$ peaks with positions of $\tau_2 = \pm k/\Delta f, k = 0, 1, \ldots, T\Delta f - 1$ and values of $M - v$. If there is a peak that encounters the mainlobe of the sinc-like function, a high grating sidelobe will be present at $f(\theta, \tau)$.

From (10) and (12), it can be seen that the same frequency step and the constant modulation bandwidth indeed cause the grating sidelobes at discrete positions τ_1, while the same frequency step also leads to the high levels of the grating sidelobes according to the sinc-like function and the in-phase items of W_v. What is more, the values of frequency step and modulation bandwidth influence the sidelobe property when the available bandwidth and the time duration are supposed fixed. The smaller the frequency step, the larger the modulation bandwidth, which results in smaller $|\tau_1|$ and larger $|\tau_2|$. Thus, the sinc-like function $|\chi_{v\Delta f}(\tau)|$ has narrower mainlobe and higher peak, and the grating lobes of $|W_v|$ will be wider and more. As a result, the grating sidelobes are closer to the mainlobe and their amplitudes become larger.

The analysis above is investigated through simulation results with $T = 100$ μs, $B = 3$ MHz, $M = 8$, $d = \lambda/2$ and $\theta = 30^\circ$ in Fig. 1, where (a) plots $|\chi_{v\Delta f}(\tau)|$, $|W_v|$ and $|f(\theta, \tau)|$ of $T\Delta f = 12$ and (b) plots those of $T\Delta f = 3$. For clarification, only $|\chi_{3\Delta f}(\tau)|$ and $|W_3(\tau)|$ are exhibited to show the principle of the grating sidelobes.

It shows that the simulation results accord with the theoretical analysis. According to the conclusions and the simulation results above, the sidelobes can be suppressed if the diversity of the frequency step or the modulation bandwidth is improved through optimization. From a practical point of view, the waveforms are usually assumed equal chirp rates, so that the complexity of hardware design and subsequent signal processing algorithm can be reduced. Therefore, the frequency steps are chosen to be optimised in this paper. Since the frequency steps are affected by the frequency codes, a joint optimisation method is proposed to optimise the frequency codes and the added phases simultaneously with ideal orthogonality. Furthermore, a modification is performed so as to eliminate the grating sidelobes thoroughly at little expense of orthogonality.

4 Joint optimisation method for OFDM LFM signal design

4.1 Description and principle of the joint optimisation method

As mentioned in Section 3, the high sidelobes of the pulse compression results are induced by the sum of the same sinc-like function $\chi_{v\Delta f}(\tau)$ and the in-phase items of W_v at $\tau_2 = \pm k/\Delta f$. It is the reason that $f_m - f_{m-v} = c_m - c_{m-v}$ $(m = v + 1, \ldots, M)$ are all equal to $v\Delta f$ with $c_m = m - (M + 1)/2$. Hence, one method for sidelobe level reduction is to increase the diversity of sinc-like functions such as breaking the conventional frequency coding sequence and changing the frequency codes to $c_m \in \{i - (M + 1)/2, i = 1, 2, \ldots, M\}$, which keeps the orthogonality. Since the spatial synthesised signal at 0° is the in-phase sum of the transmitted signals and this is not affected by the frequency coding sequence. To prevent the in-phase sum of the transmitted signals, different phases are appended to the waveforms, which can also weaken the

$$
\begin{aligned}
f(\theta, \tau) &= \int_{-\infty}^{\infty} \sum_{m=1}^{M} \mathrm{e}^{\mathrm{j}2\pi(m-1)d\sin(\theta)/\lambda} s_m(t) \sum_{i=1}^{M} \mathrm{e}^{-\mathrm{j}2\pi(i-1)d\sin(\theta)/\lambda} s_i^*(t-\tau)\,\mathrm{d}t \\
&= \int_{-\infty}^{\infty} a(t)a(t-\tau) \sum_{m=1}^{M} \mathrm{e}^{\mathrm{j}2\pi(m-1)d\sin(\theta)/\lambda} \mathrm{e}^{\mathrm{j}2\pi\left(\mu t^2/2 + f_m t\right)} \\
&\quad \sum_{i=1}^{M} \mathrm{e}^{-\mathrm{j}2\pi(i-1)d\sin(\theta)/\lambda} \mathrm{e}^{-\mathrm{j}2\pi\left[\mu(t-\tau)^2/2 + f_i(t-\tau)\right]}\,\mathrm{d}t \\
&= \sum_{m=1}^{M} \mathrm{e}^{\mathrm{j}2\pi f_m \tau} \zeta_0(\tau) \\
&\quad + \left[\sum_{m=2}^{M} \mathrm{e}^{\mathrm{j}2\pi f_{m-1}\tau} \mathrm{e}^{\mathrm{j}2\pi d\sin(\theta)/\lambda} \zeta_{f_m - f_{m-1}}(\tau) + \cdots + \sum_{m=M}^{M} \mathrm{e}^{\mathrm{j}2\pi f_{m-M+1}\tau} \mathrm{e}^{\mathrm{j}2\pi(M-1)d\sin(\theta)/\lambda} \zeta_{f_m - f_{m-M+1}}(\tau) \right] \\
&\quad + \left[\sum_{m=1}^{M-1} \mathrm{e}^{\mathrm{j}2\pi f_{m+1}\tau} \mathrm{e}^{-\mathrm{j}2\pi d\sin(\theta)/\lambda} \zeta_{f_m - f_{m+1}}(\tau) + \cdots + \sum_{m=1}^{1} \mathrm{e}^{\mathrm{j}2\pi f_{m+M-1}\tau} \mathrm{e}^{-\mathrm{j}2\pi(M-1)d\sin(\theta)/\lambda} \zeta_{f_m - f_{m+M-1}}(\tau) \right] \\
&= \sum_{m=1}^{M} \mathrm{e}^{\mathrm{j}2\pi f_m \tau} \zeta_0(\tau) + \sum_{v=1}^{M-1} R_v(\tau) + \sum_{n=1}^{M-1} Z_n(\tau)
\end{aligned}
\tag{5}
$$

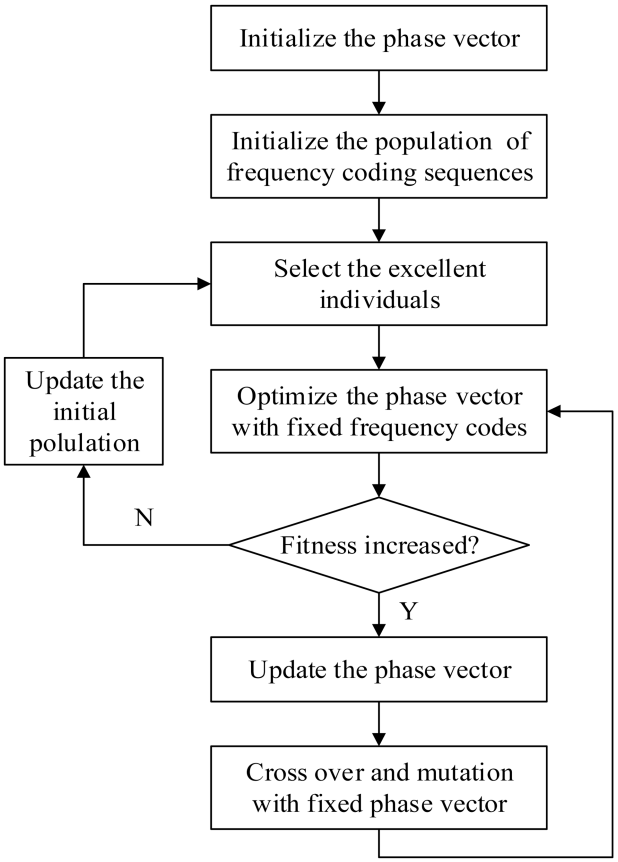

Fig. 2 *Flowchart for joint optimisation*

in-phase property of W_v. Thus, the vth term of the left sidelobes becomes

$$R_v(\tau) = \sum_{m=v+1}^{M} \mathrm{e}^{\mathrm{j}\pi(c_m + c_{m-v})\Delta f \tau} \mathrm{e}^{\mathrm{j}2\pi v d \sin(\theta)/\lambda} \mathrm{e}^{\mathrm{j}(\varphi_m - \varphi_{m-v})} \chi_{(c_m - c_{m-v})\Delta f}(\tau) \tag{13}$$

where $c_m \in \{i-(M+1)/2,\ i=1,\ 2,\ \ldots,\ M\}$ and $\varphi_m \in [0,\ 2\pi]$ are the frequency code and phase of the transmitted signal $s_m(t)$, respectively.

Aiming at sidelobe suppression, the frequency codes and the phases of transmitted signals should be chosen carefully. Since there may be some especially large sidelobes according to the criteria of integrated sidelobes, the cost function in this paper is chosen as the peak sidelobe level of the pulse compression results of the spatial synthesised signals which is as follows:

$$E = \max_{\substack{p=1,\,2,\,\ldots,\,P \\ 0<\tau\le T}} \left|f(\theta_p,\,\tau)\right| \tag{14}$$

where P is the number of target directions of interest, $0<\tau\le T$ comes from the symmetry of autocorrelation functions. The value of the cost function changes with the frequency codes and the phases. Hence, a joint optimisation method based on GA and SQP is proposed to design OFDM LFM waveform. On account of the discrete frequency codes, GA is employed to its optimisation, whereas SQP is used to choose the phases. The two variables are optimised cyclically using GA and SQP in turn.

4.2 Detailed execution of the joint optimisation method

GA is an algorithm inspired by the process of evolution in nature, which usually involves some operations such as selection, cross-over and mutation. Along with the progress, better individuals of larger fitness will be produced, whereas the worst individuals will be taken out. GA is widely used in many problems of optimisation owing to its easy operation, effective search and robustness. The carrier frequencies $\{f_m\} = \{f_0 + c_m\Delta f\} = \{f_0 + (m-((M+1)/2))\Delta f\}$ can be represented by coding sequence $\{m_1,\ m_2,\ \ldots,\ m_M\}$, called genes in the chromosome. To avoid repetition and absence of frequency codes, the coding sequences should be transformed into Grefenstette codes [30] before genetic operators.

The phase optimisation can also be realised by GA if the phases are chosen from some fixed values, but the few degrees of freedom will depress the improvement of correlation properties. To prevent this limitation, the phases are proposed to be arbitrary values in [0, 2π]. Thus, the selection of the phases should differ from that of the frequency codes, which can be described by an optimisation model as

$$\begin{aligned} &\min_{\boldsymbol{\Phi}} \max_{\substack{p=1,\,2,\,\ldots,\,P \\ 0<\tau\le T}} \left|f(\theta_p,\,\tau)\right| \\ &\text{s.t.}\quad 0 \le \varphi_m \le 2\pi \end{aligned} \tag{15}$$

where $\boldsymbol{\Phi} = [\varphi_1,\ \varphi_2,\ \ldots,\ \varphi_M]^{\mathrm{T}}$ is the phase vector of the transmitted OFDM LFM waveform. The objective function is non-convex, which makes it hard to obtain the optimum phase vector. Since (15) is a non-linear problem and SQP [28] can solve this kind of problem successfully, hence it is adopted to solve (15) in this paper.

Combining GA of frequency coding sequence optimisation and SQP of phase vector selection, the basic steps of jointly cyclic optimisation are summarised as follows:

i. *Initialisation of phase vector*: Generate M random values in [0, 2π] as the elements of the phase vector $\boldsymbol{\Phi}^0$, and treat $\boldsymbol{\Phi}^0$ as the current phase vector.
ii. *Initialisation of frequency coding sequences*: Q^0 frequency coding sequences are produced through stochastic permutations as the initial population $\mathbf{Pop}^0$.
iii. *Selection*: With the fixed phase vector $\boldsymbol{\Phi}^0$, evaluate the fitness value of each individual in $\mathbf{Pop}^0$ according to (14). Pick out Q better individuals and form a current population **Pop**.
iv. *Phase optimisation*: Sort the Q individuals according to their fitness values, and then apply SQP to the Q individuals in turn. If the better phase vector $\boldsymbol{\Phi}_b$ exists, perform updating as $\boldsymbol{\Phi}^0 = \boldsymbol{\Phi}_b$; otherwise, jump to step (vi).
v. *Cross-over and mutation*: To multiply the generation, cross-over and mutation are carried out to the current population **Pop**. The two-point cross-over is imposed on arbitrary gene segments of two individuals with probability p_c. While mutation is performed on a random individual with probability p_m, which generates a new chromosome through exchanging two genes. Then jump to step (iv). Note that simulated annealing is added to avoid trapping into a local optimum.
vi. *Updating of initial population*: When the better phase vector and frequency coding sequence cannot be found, it shows that the best individual of the current population is close to the optimum. To avoid resulting in the local optimum and accelerate the convergence, the initial population should be updated. The newly initial population $\mathbf{Pop}^0$ is generated through cross-over and mutation of the $J(J<Q)$ prior better individuals in **Pop**. Thus the range of search is broadened, and all the individuals in the newly initial population approach the optimum. Then go back to step (iii).
vii. *Termination*: GA should be stopped via searching for some generations. The optimal frequency coding sequence is the best individual in **Pop**, and the resultant phase vector is the current phase vector $\boldsymbol{\Phi}^0$. The flowchart for joint optimisation of frequency coding sequence and phase vector is shown in Fig. 2.

4.3 Modification for grating sidelobe elimination

The main drawback of OFDM LFM waveform is the high grating sidelobes in autocorrelations of spatial synthesised signals. The proposed joint optimisation method above can reduce the sidelobe

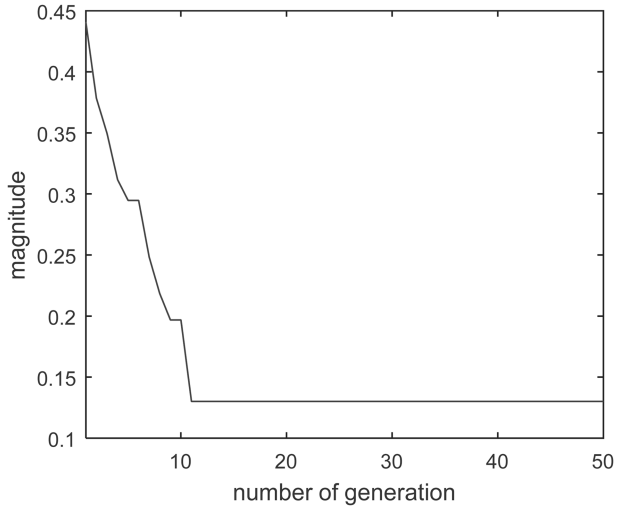

Fig. 3 *Iteration convergence*

level on the premise of orthogonality, but the sidelobes are still discrete owing to the fixed values of frequency steps. Hence, we propose a modification whose purpose is to eliminate the grating sidelobes thoroughly in this section.

In existing methods and the proposed joint optimisation method, the constraint of $\Delta f = q/T$ is imposed to guarantee the orthogonality of transmitted OFDM LFM signals. This constraint restricts the sinc-like functions to the set of $\{\chi_{-(M-1)}(\tau),\ \ldots,\ \chi_{-1}(\tau),\ \chi_1(\tau),\ \ldots,\ \chi_{M-1}(\tau)\}$, which produces the grating sidelobes of fixed positions. Thus, it is the frequency steps of special values that induce the grating sidelobes in pulse compression results. For elimination of the grating sidelobes, we make the frequency steps diverse to relax the constraint. The frequency steps are assumed to be $\{\Delta f_1,\ \Delta f_2,\ \ldots,\ \Delta f_{M-1}\}$. With the fixed first carrier frequency $f_1 = f_0 - (B - B_s)/2$, other carrier frequencies can be calculated as $f_m = f_1 + \sum_{r=1}^{m-1} \Delta f_r$, where $m = 2,\ 3,\ \ldots,\ M$ and $r = 1,\ 2,\ \ldots,\ M - 1$. Thus the sidelobe term is changed to

$$R_v(\tau) = \sum_{m=v+1}^{M} \mathrm{e}^{\mathrm{j}\pi(f_m + f_{m-v})\tau} \mathrm{e}^{\mathrm{j}2\pi v d \sin(\theta)/\lambda} \mathrm{e}^{\mathrm{j}(\varphi_m - \varphi_{m-v})} \chi_{f_m - f_{m-v}}(\tau) \quad (16)$$

where the subscript $f_m - f_{m-v} = \sum_{r=m-v}^{m-1} \Delta f_r$ varies with v and m, which has effect on the positions of sidelobes. Therefore, the sidelobes will not be discrete at some fixed positions anymore, but the problem of orthogonality arises, which leads to the non-uniform energy in space.

Considering the comparative importance of pulse compression property and orthogonality, the optimisation model should conclude these two aspects. It can be seen from (3) that the orthogonality is characterised by the covariance matrix. Thus, to ensure the orthogonality, we just need to let the covariance matrix approach the identity matrix. For sidelobe suppression and orthogonality approach, the optimisation model established based on temporal property and spatial property jointly is described as

$$\begin{aligned}
\min_{\boldsymbol{\Delta f},\ \boldsymbol{\Phi}} \quad & \max_{\substack{p = 1,\ 2,\ \ldots,\ P \\ 0 < \tau \le T}} \left| f(\theta_p,\ \tau) \right| \\
\text{s.t.} \quad & \left\| \frac{1}{T} \int_0^T \boldsymbol{S}(t) \boldsymbol{S}^{\mathrm{H}}(t)\ \mathrm{d}t - \boldsymbol{I}_M \right\|_{\mathrm{F}} \le \varepsilon \\
& \sum_{i=1}^{M-1} \Delta f_i = B - B_s \\
& \Delta f_i > 0, \quad i = 1,\ 2,\ \ldots,\ M - 1 \\
& \Delta f_i \ne q/T, \quad q = 1,\ 2,\ \ldots,\ \lceil (B - B_s)/(M - 1) \rceil \\
& 0 \le \varphi_m \le 2\pi, \quad m = 1,\ 2,\ \ldots,\ M
\end{aligned} \quad (17)$$

where $\boldsymbol{\Delta f} = [\Delta f_1,\ \Delta f_2,\ \ldots,\ \Delta f_{M-1}]^{\mathrm{T}}$ is the vector consisting of the frequency steps, $\boldsymbol{\Phi}$ is the phase vector and ε is a positive number of small value. The first constraint has effect on the orthogonality approximation and the second constraint is to ensure the modulation bandwidth B_s, which is the reason for the constant width of mainlobe. Then, the frequency steps and the phases can be obtained by SQP based on model (17).

5 Design results

In this section, we provide some design examples and simulation results to demonstrate the effectiveness of the proposed methods. As described above, the joint optimisation of frequency codes and phases based on GA and SQP is first implemented to suppress the high grating sidelobe level of pulse compression results of spatial synthesised signals. Then, the modification is performed to eliminate the grating sidelobes thoroughly. The basic parameters of GA are set as follows: the initial population contains 100 individuals, the number of individuals picked out for phase optimisation is 20, the probabilities of cross-over and mutation are 0.8 and 0.5, five prior better individuals are used to update the initial population. The value of ε in the modification is chosen as 0.2.

Assume that the OFDM LFM waveform set of $M = 8$ with half-wavelength spaced apart, $T = 100$ μs, $B = 3$ MHz and $B_s = 2.16$ MHz is designed, while another waveform of $B_s = 2.79$ MHz is also designed for comparison. Since the equal power is received in all directions as the transmitted signals are orthogonal, the directions of interest are chosen as $\{-90^\circ, -89^\circ,\ \ldots,\ 90^\circ\}$.

First, we verify the convergence of the proposed joint optimisation method. Fig. 3 plots the iteration convergence of $B_s = 2.16$ MHz. To accelerate the convergence speed, the initial phase vector is optimised in the initialisation step. It can be seen that the fitness becomes constant after 10–20 iterations, which shows good convergence characteristic.

The pulse compression properties of the spatial synthesised signals are explored in the following example. For comparison, the waveforms designed by joint optimisation and further modified are both listed; results of the conventional OFDM LFM waveforms with frequency codes $c_m = m - (M + 1)/2,\ m = 1,\ 2,\ \ldots,\ M$ [20] are also plotted. Figs. 4*a* and *b* plot the average pulse compression results of the spatial synthesised signals in all directions with $B_s = 2.16$ MHz and 2.79 MHz, respectively.

It can be seen from Fig. 4 that the average sidelobes of the waveforms obtained by joint optimisation and modification are both much lower than that of the conventional waveforms. Note that the number of the grating sidelobes in the joint optimisation method may be larger than that in the reference method in some situations. The reason is that the sinc-like functions in the proposed method may appear in different positions and the summations of them result in more small peaks. It shows that after modification, the grating sidelobes of the fixed positions do not exist anymore, but the autocorrelation peak sidelobe level has slight change compared with that of joint optimisation method. Considering the false detection is mainly caused by the high grating sidelobes, the waveforms synthesised by the proposed methods have better performance than the traditional waveforms.

The pulse compression properties of spatial synthesised signals determine the target detection performance under the circumstance of single target. While in the situation of multiple targets, the target detection is also influenced by the spatial cross-correlation functions. Figs. 5*a* and *b* show the average cross-correlations of the spatial synthesised signals with $B_s = 2.16$ MHz and 2.79 MHz, respectively.

From Fig. 5, we can see that the cross-correlation levels of the designed waveforms and that of the conventional waveforms are comparative. The reason is that the cross-correlations of the spatial synthesised signals are not considered, and hence the cross-correlation property is not improved. Similar to autocorrelations, the grating lobes of average cross-correlation functions are also eliminated by the modification, and the cross-correlation levels at non-zero delays are lower. Though the optimisations do not

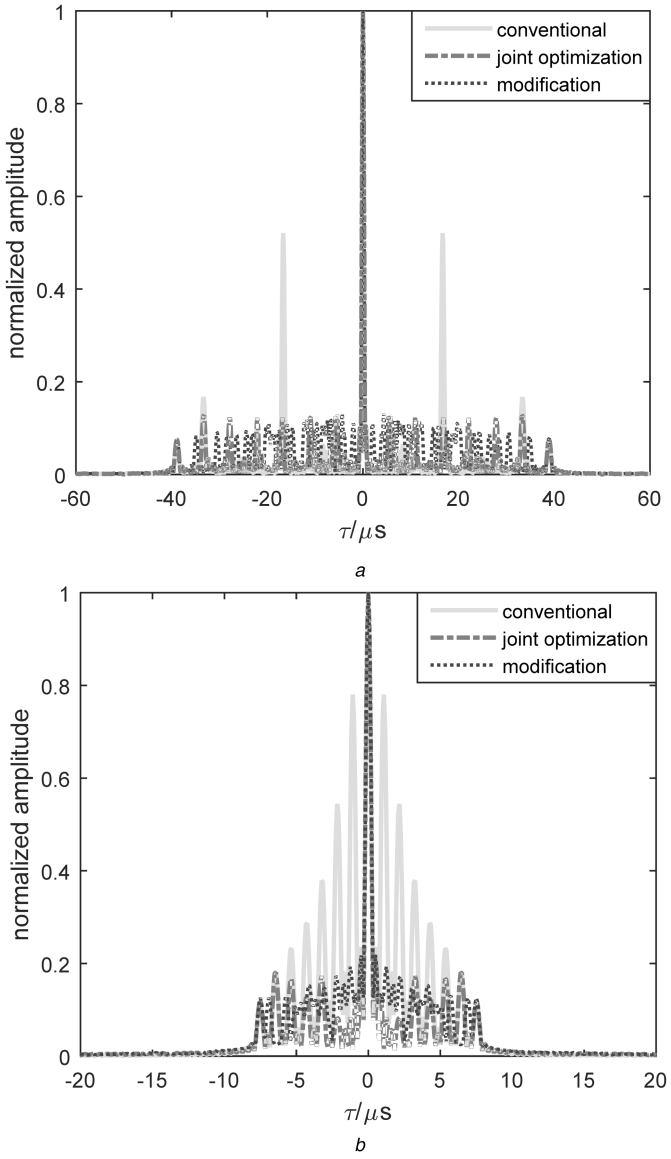

Fig. 4 *Average pulse compression results of spatial synthesised signals*
a $B_S = 2.16$ MHz
b $B_S = 2.79$ MHz

conclude the cross-correlations, the designed waveforms result in considerable performance in cross-correlation property.

To indicate the difference between joint optimisation method and the modification in orthogonality, the transmit beampatterns are shown in Fig. 6. The transmit beampatterns show that the conventional waveform and the joint optimised waveform are completely orthogonal, whereas the modified waveform does not has this property owing to the relaxation on frequency steps. Thanks to the constraint on covariance matrix, the modified waveform has approximate orthogonality, which has little influence on the range of detection for radar according to the almost omnidirectional transmit beampattern.

Applying the proposed methods for optimisation, OFDM LFM waveforms of arbitrary numbers, various time durations, varied bandwidths and different frequency steps can be designed. To analyse the performance of the designed OFDM LFM waveforms comprehensively, the correlation properties of different modulation bandwidths with $M = 8$, $T = 100$ μs and $B = 3$ MHz are listed in Table 1, which includes the maximum autocorrelation sidelobe peaks (ASPs), mean ASPs and mean cross-correlation peaks (CPs) of spatial synthesised signals. Owing to that the spatial cross-correlation with too close angles approximates the autocorrelation, the maximum CPs are not necessary to be listed or compared.

It shows that the joint optimisation and the modification both work effectively on reduction of maximum ASPs and mean ASPs with different modulation bandwidths. While on mean CPs, the modified design method acts better than the joint optimisation. Similar to the conventional waveform, the correlation properties of our designed waveforms vary with the modulation bandwidth, but the variance is more stable.

To verify the effectiveness of the proposed design methods with different parameters, the waveforms of $M = 8$, $T = 100$ μs and $B = 2$ MHz are also designed, and the related correlation performance is shown in Table 2. For comparison with correlation properties of $B = 3$ MHz, the waveforms in the same columns of Tables 1 and 2 have the same sum value of frequency steps.

Compared with Table 1, it can be seen that the correlation properties of the waveforms are concerned with the total bandwidth. For conventional waveform, the correlation properties are easily affected by the total bandwidth, whereas the effect is alleviated for our designed waveforms.

From the analysis above, we can see that the proposed methods have different improvements in correlation properties according to various parameters of the transmitted waveforms. The motivation of the proposed methods is to suppress the high grating sidelobes, so it should be emphasised that the improvement depends on the distribution of sidelobes. Thus the basic waveform parameters such as bandwidth, time duration and the transmitted signals' number all have considerable influence on the correlation properties of the

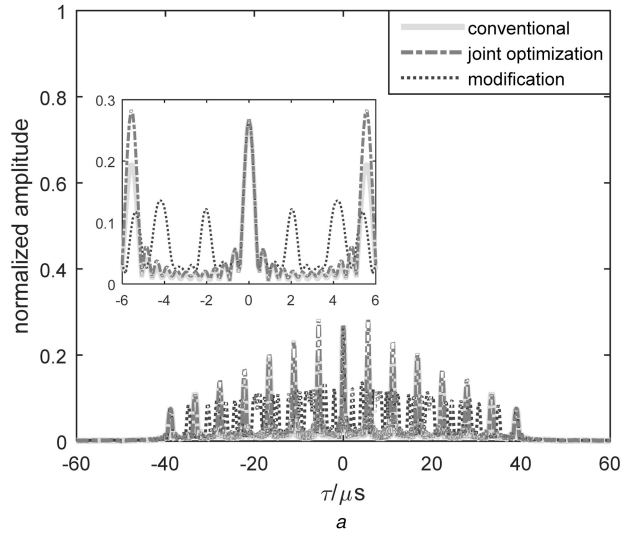

a

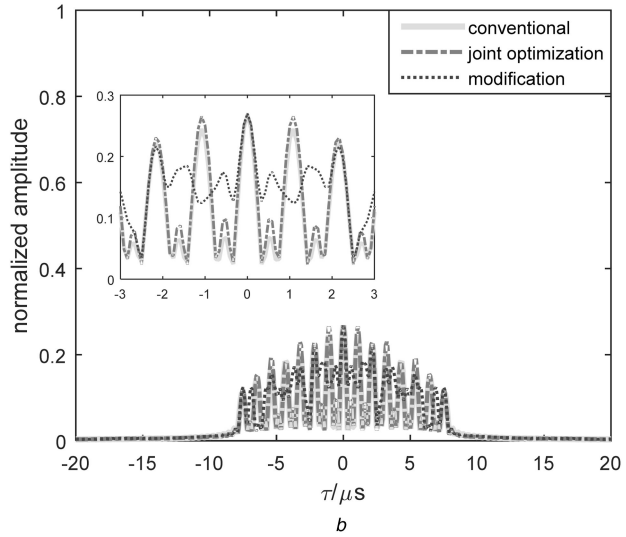

b

Fig. 5 *Average cross-correlations of spatial synthesised signals*
a $B_S = 2.16$ MHz
b $B_S = 2.79$ MHz

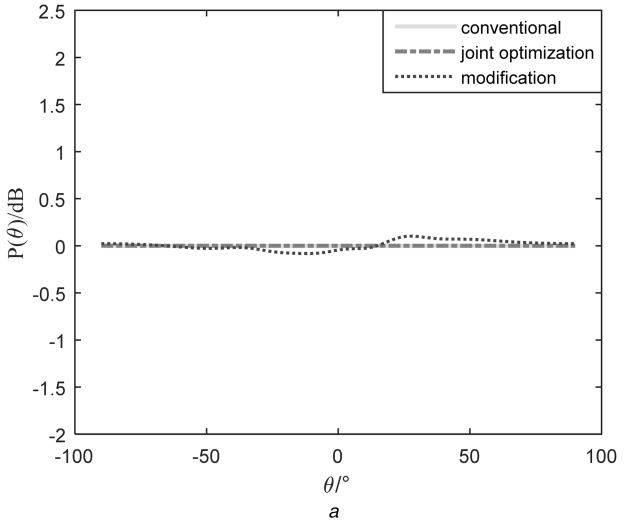

a

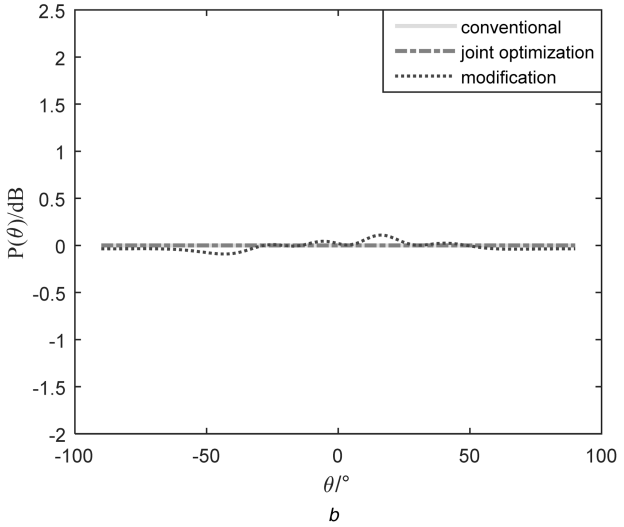

b

Fig. 6 *Transmit beampatterns*
a $B_S = 2.16$ MHz
b $B_S = 2.79$ MHz

Table 1 Correlation properties with $M = 8$, $T = 100$ μs and $B = 3$ MHz

	B_s, MHz	2.72	2.44	2.16	1.81	1.46
conventional	max ASP	0.6499	0.4133	0.5208	0.2060	0.3399
	mean ASP	0.6420	0.4102	0.5208	0.1994	0.3261
	mean CP	0.5674	0.6405	0.5341	0.6525	0.6367
joint optimisation	max ASP	0.2061	0.1745	0.1302	0.1148	0.1384
	mean ASP	0.2036	0.1724	0.1288	0.1138	0.1373
	mean CP	0.5539	0.5338	0.5292	0.5312	0.5366
modified	max ASP	0.2381	0.1766	0.1376	0.1284	0.1232
	mean ASP	0.2237	0.1748	0.1354	0.1274	0.1214
	mean CP	0.4429	0.3639	0.3527	0.3503	0.3829

Table 2 Correlation properties with $M = 8$, $T = 100$ μs and $B = 2$ MHz

	B_s, MHz	1.72	1.44	1.16	0.81	0.46
conventional	max ASP	0.4117	0.3516	0.3077	0.3620	0.2867
	mean ASP	0.3940	0.3251	0.2859	0.3546	0.2785
	mean CP	0.6569	0.6460	0.6466	0.6442	0.7006
joint optimisation	max ASP	0.1985	0.1219	0.1499	0.1540	0.1810
	mean ASP	0.1942	0.1173	0.1452	0.1519	0.1802
	mean CP	0.6033	0.5987	0.5204	0.5700	0.6517
modified	max ASP	0.2256	0.1668	0.1333	0.1248	0.2021
	mean ASP	0.2175	0.1610	0.1311	0.1201	0.2007
	mean CP	0.4226	0.3744	0.3686	0.4275	0.6124

designed OFDM LFM waveforms, but the detailed results are not listed considering the already lengthy paper.

The methods are proposed to improve the pulse compression property of spatial synthesised signals. Both the performance in sidelobes and transmit beampattern are taken into account in our design methods. The sidelobes of the modification are more uniform than that of the joint optimisation, but note that its sidelobe level is not always lower and vice versa. The transmit beampattern of the joint optimisation is ideally omnidirectional, whereas it is relaxed to the modified waveform. Thus, the two methods are comparative and should be applied according to the request of applications such as the different signal processing structures. When transmit–receive beamforming after the bank of matched filters is performed, the transmitted signals are required orthogonal strictly for ideal separation, and thus we can choose the waveform designed by the joint optimisation. The other signal processing flow is space–time matched filter after receive beamforming, in which the waveform modified with orthogonality relaxation can be used. In conclusion, both of the proposed methods can be applied to waveform design for MIMO radar, we can make a choice according to the different practice requirements.

6 Conclusion

Pulse compression property of spatial synthesised signals plays an important role in MIMO radar according to the signal processing structure. On the basis of the pulse compression analysis of spatial synthesised signals of OFDM LFM waveform, a joint optimisation method is proposed to choose the frequency codes and the phases for high grating sidelobe suppression, which results in sidelobe level reduction with ideal orthogonality. What is more, a modification is implemented, whose purpose is to eliminate the grating sidelobes thoroughly and approach the orthogonality approximately. Simulation and analysis results show that the spatial synthesised signals of the designed waveforms have better correlation properties compared with the conventional waveform.

7 References

[1] Bliss, D., Forsythe, K.: 'MIMO radar and imaging: degrees of freedom and resolution'. Proc. 38th Asilomar Conf. Signals, Systems and Computers, 2003, vol. **1**, pp. 54–59

[2] Forsythe, K.W., Bliss, D.W., Fawcett, G.S.: 'Multiple-input multiple-output (MIMO) radar: performance issues'. Proc. 38th Asilomar Conf. Signals, Systems and Computers, 2004, pp. 310–315

[3] Li, J., Stoica, P.: 'MIMO radar with colocated antennas', *IEEE Signal Process. Mag.*, 2007, **24**, (5), pp. 106–114

[4] Khan, H.A., Edwards, D.J.: 'Doppler problems in orthogonal MIMO radars'. Proc. IEEE Radar Conf., 2006, vol. **1**, pp. 244–247

[5] Tang, J., Zhang, N., Ma, Z.K.*, et al.*: 'Construction of Doppler resilient complete complementary code in MIMO radar', *IEEE Trans. Signal Process.*, 2014, **62**, (18), pp. 4704–4712

[6] Baghel, V., Panda, G.: 'Development and performance evaluation of generalized Doppler compensated adaptive pulse compression algorithm', *IET Radar Sonar Navig.*, 2014, **8**, (4), pp. 297–306

[7] Deng, H.: 'Polyphase code design for the orthogonal netted radar systems', *IEEE Trans. Signal Process.*, 2004, **52**, (11), pp. 3126–3135

[8] Liu, B.: 'Orthogonal discrete frequency-coding waveform set design with minimized autocorrelation sidelobes', *IEEE Trans. Aerosp. Electron. Syst.*, 2009, **45**, (4), pp. 1650–1657

[9] Wang, W.Q.: 'Large time-bandwidth product MIMO radar waveform design based on chirp rate diversity', *IEEE Sens. J.*, 2015, **15**, (2), pp. 1027–1034

[10] Chen, C.Y., Vaidyanathan, P.P.: 'MIMO radar ambiguity properties and optimization using frequency-hopping waveforms', *IEEE Trans. Signal Process.*, 2008, **56**, (12), pp. 5926–5936

[11] Zhao, D.H., Wei, Y.S.: 'Adaptive gradient search for optimal sidelobe design of hopped-frequency waveform', *IET Radar Sonar Navig.*, 2014, **8**, (4), pp. 282–289

[12] Gao, C.C., Teh, K.C., Liu, A.F.: 'Orthogonal frequency diversity waveform with range-Doppler optimization for MIMO radar', *IEEE Signal Process. Lett.*, 2014, **21**, (10), pp. 1201–1205

[13] Dormet, B.J., Longstaff, I.D.: 'Combining MIMO radar with OFDM communications'. Proc. Third European Radar Conf., 2006, vol. **1**, pp. 37–40

[14] Sen, S., Tang, G.G., Nehorai, A.: 'Multiobjective optimization of OFDM radar waveform for target detection', *IEEE Trans. Signal Process.*, 2011, **59**, (2), pp. 639–652

[15] Sen, S., Nehorai, A.: 'Adaptive design of OFDM radar signal with improved wideband ambiguity function', *IEEE Trans. Signal Process.*, 2010, **58**, (2), pp. 928–933

[16] Kim, J., Younis, M., Moreira, A.*, et al.*: 'A novel OFDM chirp waveform scheme for use of multiple transmitters in SAR', *IEEE Geosci. Remote Sens. Lett.*, 2013, **10**, (3), pp. 568–572

[17] Kim, J., Younis, M., Moreira, A.*, et al.*: 'Spaceborne MIMO synthetic aperture radar for multimodal operation', *IEEE Trans. Geosci. Remote Sens.*, 2015, **53**, (5), pp. 2453–2466

[18] Wang, W.Q.: 'MIMO SAR OFDM chirp waveform diversity design with random matrix modulation', *IEEE Trans. Geosci. Remote Sens.*, 2015, **53**, (3), pp. 1615–1625

[19] Dai, X.Z., Xu, J., Ye, C.M.*, et al.*: 'Low-sidelobe HRR profiling based on the FDLFM-MIMO radar'. Proc. Asian and Pacific Conf. Synthetic Aperture Radar, Huangshan, China, 2007, pp. 132–135

[20] Cheng, F., He, Z.S., Liu, H.M.*, et al.*: 'The parameter setting problem of signal OFDM-LFM for MIMO radar'. Proc. IEEE Int. Conf. Communications, Circuits and Systems, 2008, pp. 876–880

[21] Levanon, N.: 'Stepped-frequency pulse-train radar signal', *Proc. IEE Radar Sonar Navig.*, 2002, **149**, (6), pp. 297–309

[22] Maron, D.E.: 'Non-periodic frequency-jumped burst waveforms'. Proc. IEE Int. Radar Conf., 1987, pp. 484–488

[23] Maron, D.E.: 'Frequency-jumped burst waveforms with stretch processing'. Proc. IEEE Int. Radar Conf., 1990, pp. 274–279

[24] Rabideau, D.J.: 'Nonlinear synthetic wideband waveforms'. Proc. IEEE Radar Conf., 2002, pp. 212–219

[25] Gladkova, I., Chebanov, D.: 'Grating lobes suppression in stepped-frequency pulse train', *IEEE Trans. Aerosp. Electron. Syst.*, 2008, **44**, (4), pp. 1265–1275

[26] Tang, K.S., Man, K.F., Kwong, S.*, et al.*: 'Genetic algorithms and their applications', *IEEE Signal Process. Mag.*, 1996, **13**, (6), pp. 22–37

[27] Liu, B., He, Z.S., He, Q.: 'Optimization of orthogonal discrete frequency-coding waveform based on modified genetic algorithm for MIMO radar'. Proc. IEEE Int. Conf. Communications, Circuits and Systems, Kokura, 2007, pp. 966–970

[28] Rau, N.: '*Optimization principles: practical applications to the operation and markets of the electric power industry*' (Wiley-IEEE Press, 2003), pp. 177–243

[29] Davis, M.S., Lanterman, A.D.: 'Minimum integrated sidelobe ratio filters for MIMO radar', *IEEE Trans. Aerosp. Electron. Syst.*, 2015, **51**, (1), pp. 405–416

[30] Grefenstette, J.J., Gopal, R., Rosmaita, B.J.*, et al.*: 'Genetic algorithms for the traveling salesman problems'. Proc. Int. Conf. Genetic Algorithms and their Applications, Carnegie-Mellon University, 1985, pp. 160–168